

Solving a coupled fluid-solid system with PINNs

Davide Staub

Abstract

This study initially pursued resolving a complex mixed physics problem using Physics Informed Neural Networks (PINNs), revealing significant challenges in the process. In addressing the component problems independently, the acoustic wave equation was resolved efficiently, while the elastic wave equation emerged as a more complex issue. Particularly, capturing accurate initial conditions emerged as a significant challenge, despite our exploration of various approaches, including weakly constrained, hard-constrained, and analytical methods. We employed multiple strategies such as curriculum-based learning to mitigate these issues, with limited success. While PINNs hold the potential to efficiently address complex physics problems, our study sheds light on key areas that need further investigation, particularly the accurate representation of initial conditions and addressing issues of persistent loss stagnation.

1 Introduction

Understanding the behavior of coupled seismic and acoustic waves within solid-fluid systems holds potential for numerous applications, spanning from planetary science to terrestrial hazard prediction. Enhancing our knowledge of this coupling could refine the performance of sensors at these interfaces, with implications for initiatives as diverse as Mars mission payload analyses and proposed Venus explorations. While established numerical codes such as SPECFEM2D-DG [2] currently offer solutions to these complex problems, these methodologies can be computationally demanding, particularly when involving multiple sources of seismic activity. In this semester thesis, we embark on an exploratory journey to apply Physics-Informed Neural Networks (PINNs) to tackle this coupled seismic-acoustic challenge. Although our approach is in its early stages, our aim is to potentially alleviate some of the computational burdens inherent in traditional numerical simulations.

2 Contribution

This paper encapsulates the work and results of my Semester thesis undertaken at Oxford University, as part of the "Computational Science and Engineering" Master's program at ETH Zurich. Our exploration centered on the intricate

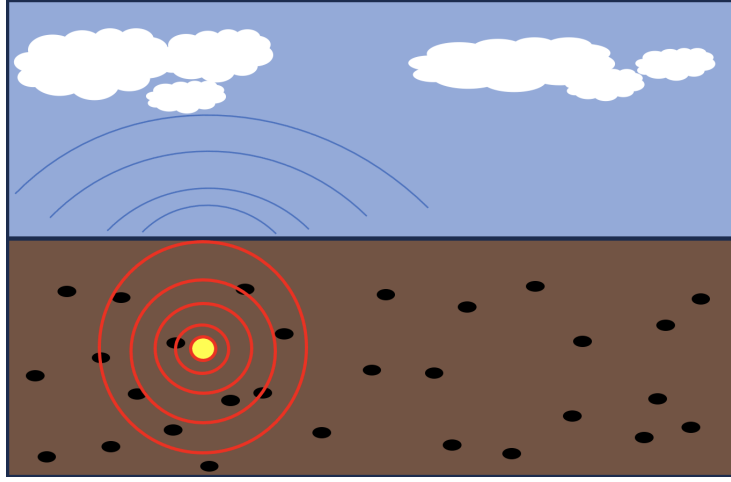


Figure 1: Schematics of a coupled solid-fluid system with a seismic wave propagating through the solid part and later as an acoustic wave through the fluid medium, which in this case is depicted as the atmosphere

challenge of solving the seismic-acoustic wave propagation problem using PINNs. Recognizing that this complex issue remains an open problem, this work delineates our methodological explorations, primarily focusing on handling the elastic and acoustic wave equations separately. Particular attention was paid to the initial conditions, which demanded extensive experimentation. While notable progress was made, further research is needed to fully address the problem's complexities.

3 Method

3.1 Governing equations

The first goal of this thesis was to solve the mixed physics problem comprised of a solid and fluid state with a seismic wave initiated in the solid part and then propagating through both the solid and fluid phases. Our first approach was to translate the equations present in the paper [2]. They are as follows. The solid domain is considered to be heterogeneous, linear, and viscoelastic. The governing equation is the linear wave equation, which, for this setting is known

as the elastodynamics system.

$$\begin{aligned}
\rho^s \partial_t^2 \mathbf{u}^s &= \nabla \cdot \Sigma^s + F^s \\
\Sigma^s &= C^U : \varepsilon - \sum_{l=1}^L \mathbf{R}^l \\
\varepsilon &= \frac{1}{2} (\nabla \mathbf{u} + (\nabla \mathbf{u})^T) \\
\forall 1 \leq l \leq L, \partial_t \mathbf{R}^l &= \frac{1}{\tau^{S^l}} (-\mathbf{R}^l + \delta c^l : \varepsilon)
\end{aligned} \tag{1}$$

where ρ^s is the solid density, \mathbf{u}^s is the solid displacement, Σ^s is the solid stress tensor, and F^s are the external forces applied on the solid. In our case the external forces F^s need not be present in the equation as they are handled by an initial condition. Furthermore, we assumed a purely elastic medium, which does not experience any form of dissipation or attenuation, so there is no need for the auxiliary variables R^l . Therefore the equations simplify to:

$$\begin{aligned}
\rho^s \partial_t^2 \mathbf{u}^s &= \nabla \cdot \Sigma^s \\
\Sigma^s &= C^U : \varepsilon \\
\varepsilon &= \frac{1}{2} (\nabla \mathbf{u} + (\nabla \mathbf{u})^T)
\end{aligned} \tag{2}$$

Further assuming the material to be isotropic results in a readily available computation of the stress tensor.

$$\Sigma_{ij}^s = C_{ijkl} \varepsilon_{kl} \tag{3}$$

$$C_{ijkl} = \lambda \delta_{ij} \delta_{kl} + \mu \delta_{ik} \delta_{jl} + \delta_{il} \delta_{jk} \tag{4}$$

where δ_{jl} is the Kronecker-delta, and λ and μ are the Lamé constants. Therefore the overall governing equations for the solid state are given by:

$$\begin{aligned}
\rho^s \partial_t^2 \mathbf{u}^s &= \nabla \cdot \Sigma^s \\
\Sigma_{ij}^s &= C_{ijkl} \varepsilon_{kl} \\
\varepsilon &= \frac{1}{2} (\nabla \mathbf{u} + (\nabla \mathbf{u})^T) \\
C_{ijkl} &= \lambda \delta_{ij} \delta_{kl} + \mu \delta_{ik} \delta_{jl} + \delta_{il} \delta_{jk}
\end{aligned} \tag{5}$$

For the fluid state, they used the linearized Navier-Stokes equation (LNS).

$$\partial_t \mathbf{U} + \nabla \cdot \Sigma^c(\mathbf{U}) = \nabla \cdot \Sigma^d(\mathbf{U}) + \mathbf{G}(\mathbf{U}) \tag{6}$$

$$\mathbf{U}(t, x) = \begin{pmatrix} \rho' \\ \rho_0 \mathbf{v}' \\ E' \end{pmatrix} \tag{7}$$

$$\boldsymbol{\Sigma}^c(\mathbf{U}(t, x)) = \begin{pmatrix} \rho_0 \mathbf{v}' + \rho' \mathbf{v}_0 \\ \rho_0 \mathbf{v}_0 \otimes \mathbf{v}' + p' I \\ (E_0 + p_0) \mathbf{v}' + (E' + p') \mathbf{v}_0 \end{pmatrix} \quad (8)$$

$$\boldsymbol{\Sigma}^d(\mathbf{U}(t, x)) = \begin{pmatrix} 0 \\ \Sigma_v(\mathbf{v}') \\ \Sigma_v(\mathbf{v}_0) \mathbf{v}' + \Sigma_v(\mathbf{v}') \mathbf{v}_0 + \kappa \nabla T' \end{pmatrix} \quad (9)$$

$$\mathbf{G}(\mathbf{U}(t, x)) = \begin{pmatrix} 0 \\ \rho' \mathbf{g} - \rho' \partial_t(\mathbf{v}_0) - ((\rho_0 \mathbf{v}' + \rho' \mathbf{v}_0) \cdot \nabla) \mathbf{v}_0 \\ \mathbf{g} \cdot (\rho_0 \mathbf{v}' + \rho' \mathbf{v}_0) \end{pmatrix} \quad (10)$$

$\mathbf{U}(t, x)$ is the state vector that encodes the perturbations on constitutive variables: $\rho'(t, x)$ the density perturbation, $\mathbf{v}'(t, x)$ the velocity perturbation, and $E'(t, x)$ the energy density perturbation. $(\rho_0(x), \mathbf{v}_0(x), E_0(x))$ are their static counterparts, that do not depend on time. Similarly, p' is the pressure perturbation and p_0 is the static pressure. Σ_c gathers the convective terms of the stress tensor whereas Σ_d collects its diffusive terms. \otimes denotes the tensor product. I is the identity matrix. $\Sigma_v(t, x)$ is the Navier–Stokes viscous stress tensor, given by

$$\Sigma_v(\mathbf{v}) = \lambda(\nabla \cdot \mathbf{v})I + \mu(\nabla \mathbf{v} + (\nabla \mathbf{v})^\mathbf{T}) \quad (11)$$

Where $\mu(x)$ is the dynamic viscosity, and $\lambda(x)$ is the second viscosity. $\kappa(x)$ is the thermal conductivity of the fluid. $T'(t, x)$ is the temperature perturbation. $\mathbf{g}(x)$ is the full acceleration of gravity. For the solid-fluid coupling boundary conditions, the reader is referred to [2]. Even though this mixed physics problem was successfully implemented in a PINNs framework, we quickly realized that the governing equations for the fluid imposed a very difficult learning task for the neural network. Therefore we decided to drastically simplify the governing equations for the fluid and assume that the underlying dynamics are given by the acoustic wave equation instead which is given by:

$$\nabla^2 u^f = \frac{1}{v^2} \partial_t^2 u^f \quad (12)$$

where $u(\mathbf{x}, t)$ is the wavefield and $\mathbf{v}(\mathbf{x})$ is the velocity. For the solid-fluid coupling, we used the following boundary conditions:

$$\begin{aligned} \boldsymbol{\Sigma}^s \cdot \mathbf{n} &= \boldsymbol{\Sigma}^f \cdot \mathbf{n} \\ \boldsymbol{\Sigma}^s \cdot \mathbf{t} &= 0 \\ \boldsymbol{\Sigma}^f \cdot \mathbf{t} &= 0 \\ (\mathbf{u}^f &= \mathbf{u}^s) \end{aligned} \quad (13)$$

Where the first of these three equations represents the balance of normal stress at the interface between the fluid and the solid. Here, $\boldsymbol{\Sigma}^s$ and $\boldsymbol{\Sigma}^f$ represent the stress tensors in the solid and fluid respectively, and \mathbf{n} represents the normal

vector to the interface. The second and third equations represent the condition of zero tangential stress at the interface in the solid and fluid respectively. This implies that there are no shear forces acting along the boundary in either medium. Here, \mathbf{t} represents the tangential vector to the interface. The final equation represents the kinematic continuity condition at the interface. It states that the displacement of the fluid \mathbf{u}^f is equal to the displacement of the solid \mathbf{u}^s at the interface, meaning the fluid and solid move together without slipping. This condition is put in parentheses as it is implicitly satisfied due to the choice of a continuous activation function of the neural network. Therefore, the overall governing equations of our mixed physics problem are given by equations 5 12 and 13.

3.2 Model setup

In order for the model to learn the underlying physics presented in 5 12 and 13 a suitable Loss function must be constructed. In this case, the Loss function consists of three terms

$$L = L_S + L_F + L_B \quad (14)$$

where L_S is the solid loss, L_F the fluid loss and L_B the boundary loss. The solid loss is given by

$$L_S = \frac{1}{N_S} \sum_{i=0}^{N_S} \left\| \rho^s \frac{\partial^2 NN(x_i, t_i; \theta)}{\partial t^2} - \nabla \cdot \Sigma_i^s(NN(x_i, t_i; \theta)) \right\|^2, \quad (15)$$

where $\Sigma_i^s(NN(x_i, t_i; \theta))$ can readily be compute as seen in equation 3 using

$$\varepsilon = \frac{1}{2} (\nabla NN(\mathbf{x}_i, t_i; \theta) + (\nabla NN(\mathbf{x}_i, t_i; \theta))^T). \quad (16)$$

where $NN(\mathbf{x}_i, t_i; \theta)$ represents the prediction of the neural network at location (\mathbf{x}_i, t_i) with network parameters θ . The fluid loss is given by

$$L_F = \frac{1}{N_F} \sum_{i=0}^{N_F} \left\| \nabla^2 NN(x_i, t_i; \theta) - \frac{1}{v^2} \frac{\partial^2 NN(x_i, t_i; \theta)}{\partial t^2} \right\| \quad (17)$$

And finally, the boundary loss is given by

$$L_{boundary} = L_n + L_{tf} + L_{ts}, \quad (18)$$

where L_n , L_{tf} , and L_{ts} represent the mean square residuals between the predicted and expected values for the normal stress, tangential fluid stress, and tangential solid stress, respectively. These can be expressed as:

$$L_n = \frac{1}{N_{boundary}} \sum_{i=0}^{N_{boundary}} \left\| \Sigma_i^s(NN(x_i, t_i; \theta)) \cdot \mathbf{n} - \Sigma_i^f(NN(x_i, t_i; \theta)) \cdot \mathbf{n} \right\|^2, \quad (19)$$

$$L_{tf} = \frac{1}{N_{boundary}} \sum_{i=0}^{N_{boundary}} \|\Sigma_i^f(NN(x_i, t_i; \theta)) \cdot \mathbf{t}\|^2, \quad (20)$$

$$L_{ts} = \frac{1}{N_{boundary}} \sum_{i=0}^{N_{boundary}} \|\Sigma_i^s(NN(x_i, t_i; \theta)) \cdot \mathbf{t}\|^2. \quad (21)$$

In the context of these equations, $\Sigma_i^s(NN(x_i, t_i; \theta))$ and $\Sigma_i^f(NN(x_i, t_i; \theta))$ correspond to the stress tensors in the solid and fluid predicted by the neural network at location (x_i, t_i) . Meanwhile, \mathbf{n} and \mathbf{t} represent the normal and tangential vectors at the fluid-solid interface, respectively. These loss terms ensure that the network finds a solution that adheres to the underlying physics as defined by equations 5, 12, and 13.

However, to guide the network towards a unique non-zero solution, it is imperative to also enforce an initial condition. Given the significant time invested in identifying a suitable method to handle the initial condition, we dedicate a separate section to this endeavor.

3.3 Initial Condition Handling

We explored three distinct approaches to enforce the neural network's adherence to the initial conditions. The first and simplest strategy involves defining a soft constraint through the addition of an extra loss term, L_{init} , to the total loss L . It is imperative to construct L_{init} such that the neural network learns to conform to the initial condition. In our specific scenario, we assumed the initial displacement field to be a Gaussian distribution with a mean (μ) and standard deviation (σ).

$$\mathbf{u}(\mathbf{x}, 0) = e^{-\frac{1}{2}(\|\mathbf{x} - \mu\|/\sigma)^2} \quad (22)$$

Therefore, L_{init} is given by:

$$L_{init} = \frac{1}{N_{init}} \sum_{i=0}^{N_{init}} \|NN(\mathbf{x}_i, 0; \theta) - e^{-\frac{1}{2}(\|\mathbf{x}_i - \mu\|/\sigma)^2}\|^2 \quad (23)$$

The subsequent two methods we investigated enforced the initial condition as a hard constraint. The first of these methods strictly adheres to the boundary conditions by incorporating the neural network into a solution Ansatz [3]:

$$\hat{u}(x, t; \theta) = \phi(15(-t - 0.75))e^{-\frac{1}{2}(\frac{\|x - \mu\|}{\sigma})^2} + \tanh^2(5(t + 1))NN(x, t; \theta) \quad (24)$$

In this formulation, $\hat{u}(x, t; \theta)$ denotes the network prediction for the displacement field. By this design, the initial conditions specified in equation 22 are automatically met at $t = 0$, effectively transforming our prior constrained optimization problem into an unconstrained one [3]. The role of $\phi(15(-t - 0.75))$ is to gradually deactivate the enforcement of the initial conditions while $\tanh^2(5(t + 1))$ is employed to activate the predictions from the neural network.

Our final strategy for handling the initial conditions shares similarities with the second one, as it also integrates the neural network into a solution Ansatz. However, a key distinction lies in the enforcement of a time-dependent analytical solution $\bar{u}(x, t)$, a representation of the seismic wave, as opposed to a simple Gaussian at $t = 0$.

$$\bar{u}(x, t) = \frac{1}{4\pi\rho\alpha^3} A^{FP} \frac{1}{r} \dot{M}_0(t - \frac{r}{\alpha}) + \frac{1}{4\pi\rho\beta^3} A^{FS} \frac{1}{r} \dot{M}_0(t - \frac{r}{\beta}) \quad (25)$$

Where r is the radial distance to the source location and ρ is the density. α is the so-called p-wave speed of the seismic wave, which can be derived from the Lamé constants as

$$\alpha = \sqrt{\left(\frac{\lambda + 2\mu}{\rho}\right)} \quad (26)$$

and β is the s-wave speed which is given by

$$\beta = \sqrt{\left(\frac{\mu}{\rho}\right)} \quad (27)$$

\dot{M}_0 is the first time derivative of the moment-function which is a measure of the total energy released by an earthquake. More specifically, the moment function is typically a time-dependent function describing the release of seismic energy over the duration of an earthquake event. We chose to model \dot{M}_0 simply as Gaussian pulse function

$$\dot{M}_0 = \frac{M_0}{T^2} \left(t - \frac{3T}{2}\right) e^{-\left(\frac{(t - \frac{3T}{2})^2}{T^2}\right)} \quad (28)$$

Here, T controls the duration of the earthquake event, while M_0 acts as a scaling factor for the event's amplitude. Two additional parameters, A^{FP} and A^{FS} , are calculated by given equations, each depending on the angles θ and ϕ . A visual representation of these angles is offered in Figure 2. A^{FP} is given by

$$A^{FP} = \sin 2\theta \cos \phi \hat{\mathbf{r}} \quad (29)$$

and A^{FS} is given by

$$A^{FS} = \cos 2\theta \cos \phi \hat{\boldsymbol{\theta}} - \cos \theta \sin \phi \hat{\boldsymbol{\phi}} \quad (30)$$

Since this analytical equation is valid only near the origin of the initial displacement field spike - both spatially and temporally - we necessitate a suitable function that controls its activation and deactivation and takes into account the spatial component:

$$\hat{u}(x, t; \theta) = \alpha(x, t) \bar{u}(x, t) + (1 - \alpha(x, t)) NN(x, t; \theta) \quad (31)$$

$$\alpha(x, t) = \exp(-\lambda^t t) \cdot \exp\left(-\frac{\lambda^x \cdot \|x - \mu\|^2}{2r^2}\right) \quad (32)$$

In these equations, $\hat{u}(x, t; \theta)$ again represents the network prediction, now comprising both the neural network output and the analytical solution. The activation/deactivation function, $\alpha(x, t)$, operates like a Gaussian in both space and time, with λ^t and λ^x representing the temporal and spatial decay rates.

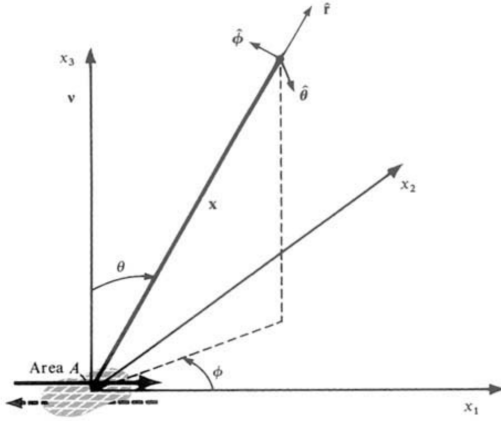


Figure 2: Representation of the coordinate system and angles. Take note that although the image showcases a 3D problem, our study is grounded in a 2D context. To reconcile this, we've fixed θ at 45° . Figure taken from [1]

4 Model setup and training strategy

Each sample fed into the neural network comprises x , y , and t components, with the network outputting the displacement field $u = (u_x, u_y)$. Given that this project is still in the developmental stages, it's premature to definitively identify the optimal hyperparameters and network architecture. Nevertheless, some fundamental choices for network architecture remained constant throughout our experiments. In line with common practices for Physics-Informed Neural Networks (PINNs), we used a straightforward feed-forward network architecture. The tanh function was selected as the activation function for all hidden layers, while a linear activation function was used for the final output layer. During training, we employed the LBFGS optimizer as it displayed faster and more stable convergence compared to the ADAM optimizer. To accommodate the tanh activation function, the weights were initialized using the Xavier initialization method. In the same vein, we scaled all input values (\mathbf{x}, t) to the Network within the range $[-1, 1]$. For the optimization process, we found full batch optimization to significantly outperform any smaller batch size. Fortunately, the training sets for the corresponding loss functions can be conveniently constructed, eliminating the need for generating training data from finite-difference simulations.

5 Results

Our initial endeavor was to tackle the full mixed physics problem. However, it became readily apparent that the network struggled significantly with learning

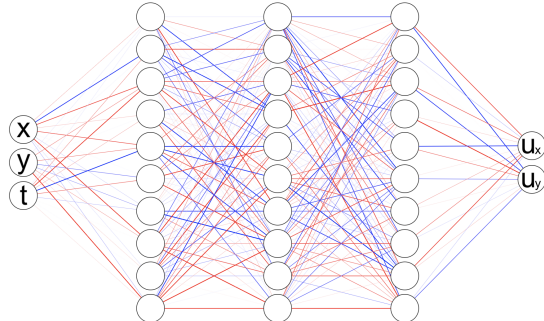


Figure 3: Sketch of the model architecture, in truth, the hidden-layer size is much larger, usually consisting of up to 512 neurons

the underlying physics. We explored various techniques to surmount this hurdle, including the application of curriculum-based learning. In this approach, points close in time to the starting point were first fed to the network, and later time points were subsequently added. The visual outcome of this effort, alongside the associated training loss, is illustrated in Figures 4 and 5.

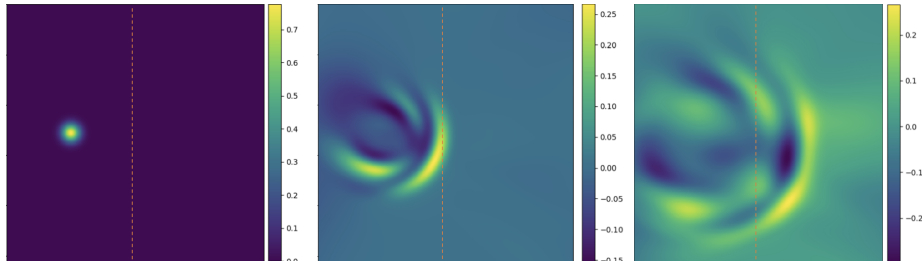


Figure 4: Neural network prediction of the mixed physics problem at $t = -1, t = 0$ and $t = 1$. The dashed red line represent the fluid-solid boundary

As illustrated, the training loss remained prohibitively high. Consequently, we concluded that a prudent first step might be to solve the uncoupled problem—addressing the elastic and acoustic wave equations separately through Physics-Informed Neural Networks (PINNs).

Previous works, such as [3], have already demonstrated successful solutions to the acoustic wave equation using PINNs. Unsurprisingly, the stand-alone acoustic wave equation was solved without any significant challenges by the network. For both weakly or strongly constrained initial conditions, the network effectively solved the acoustic wave equation. Moreover, our findings suggest that employing a hard-constrained ansatz expedited network convergence.

Resolving the elastic wave equation proved to be a far more challenging task

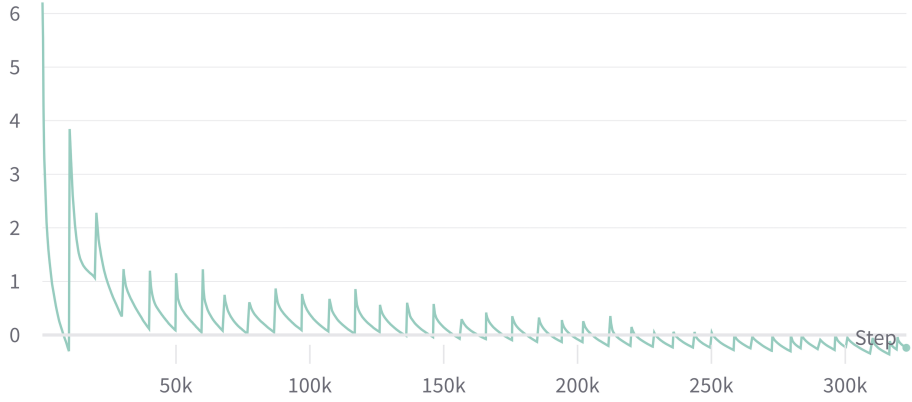


Figure 5: Training loss for the mixed physics problem.

and remains a work in progress. Utilizing the weakly constrained method to manage the initial condition was largely unsuccessful, as the network failed to accurately represent the initial condition. However, our non-analytical hard constraint approach yielded more promising results, as demonstrated in Figure 6. Notwithstanding these advances, it is apparent that the solution is still not entirely correct. For instance, an asymmetry in wave propagation is discernible right after the start in the second picture—an error that propagates as time advances.

We conjecture that this issue may stem from the treatment of the initial condition or the network’s fixation on a non-optimal solution. Figure 7 clearly indicates that, after an initial descent, the loss plateaus at a relatively high value. Although this could potentially be attributed to the vanishing gradient problem, further examination is necessary to ascertain the root cause of this phenomenon.

Despite these challenges, it is encouraging to observe the physically correct propagation of the incorrect initial wave, including discernible p and s waves. This result bolsters our confidence in the eventual successful resolution of the elastic wave equation using PINNs, albeit with additional work.

In an effort to rectify the initial condition issue, we experimented with an analytical hard constraint approach, hypothesizing that providing the network with more information could result in a more accurate solution and faster convergence. However, tuning the parameters of the activation/deactivation functions and the analytical solution to ensure that this initial condition method works well proved challenging, requiring additional investigation.

To alleviate the propagation of the initial time error, curriculum-based learning was implemented. This method ensured that time points close to the initial condition were learned first, thus respecting the causality of the PDE. However, the application of this time marching scheme resulted in substantial oscillations in the loss function, as if the network was discarding previously learned infor-

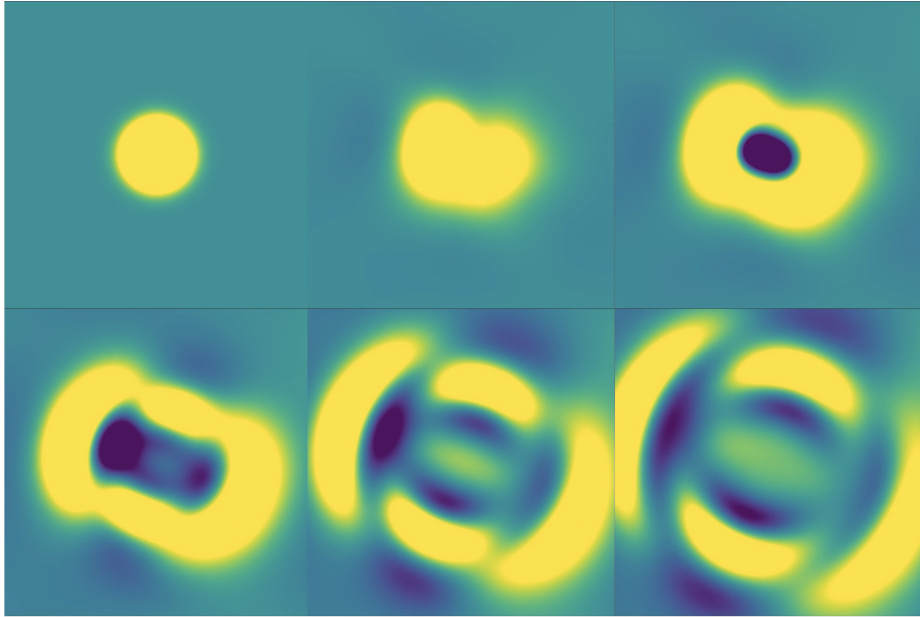


Figure 6: Neural network prediction of the elastic wave equation at times between $t = -1$ and $t = 1$.

mation with the addition of each new training point. This anomaly warrants further exploration.

6 Future Work

Moving forward, our efforts will be focused on improving the handling of initial conditions, using both analytical and non-analytical methods. We aim to enhance our curriculum-based learning strategy, ensuring the network retains its prior learning as we introduce new training data. A central objective will be to efficiently solve the elastic wave equation. Our success in this area will set the stage for addressing the more challenging mixed physics problem. We also intend to investigate the root cause of the high training loss, with a suspicion that the vanishing gradient issue may be involved. Additionally, the implementation of a test loss measure, using Finite Difference simulations as a benchmark, will provide a more comprehensive evaluation of our models. Lastly, while PINNs remain our core methodology, we will also look into other approaches which incorporate data into the learning process. This blend of techniques could potentially improve our capability to tackle intricate physical scenarios.

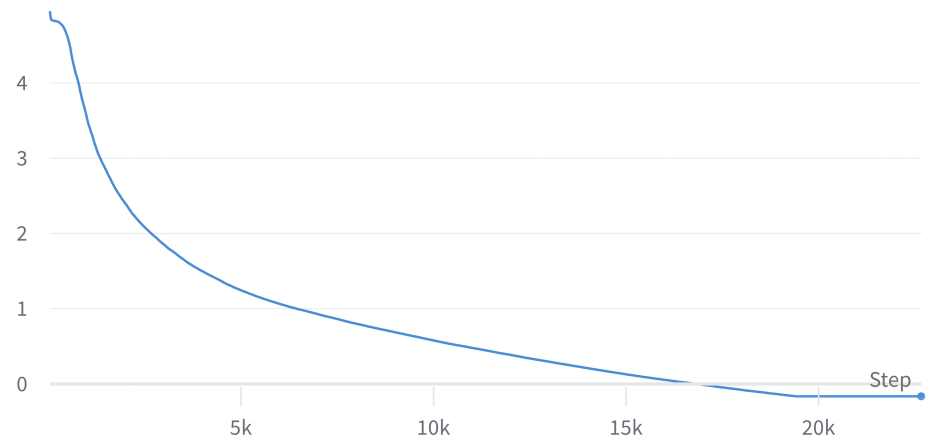


Figure 7: Training loss for the elastic wave equation.

References

- [1] Paul G. Richards Keiiti Aki. *Quantitative Seismology, 2nd Edition*. University Science Books Mill Valley, California, 2002.
- [2] Léo Martire et al. “SPECFEM2D-DG, an open-source software modelling mechanical waves in coupled solid–fluid systems: the linearized Navier–Stokes approach”. In: *Geophysical Journal International* (2021).
- [3] Benjamin Moseley, A. Markham, and Tarje Nissen-Meyer. “Finite Basis Physics-Informed Neural Networks (FBPINNs): a scalable domain decomposition approach for solving differential equations”. In: *ArXiv* abs/2107.07871 (2021).

Eigenständigkeitserklärung

Die unterzeichnete Eigenständigkeitserklärung ist Bestandteil jeder während des Studiums verfassten Semester-, Bachelor- und Master-Arbeit oder anderen Abschlussarbeit (auch der jeweils elektronischen Version).

Die Dozentinnen und Dozenten können auch für andere bei ihnen verfasste schriftliche Arbeiten eine Eigenständigkeitserklärung verlangen.

Ich bestätige, die vorliegende Arbeit selbständig und in eigenen Worten verfasst zu haben. Davon ausgenommen sind sprachliche und inhaltliche Korrekturvorschläge durch die Betreuer und Betreuerinnen der Arbeit.

Titel der Arbeit (in Druckschrift):

Verfasst von (in Druckschrift):

Bei Gruppenarbeiten sind die Namen aller Verfasserinnen und Verfasser erforderlich.

Name(n):

Vorname(n):

Ich bestätige mit meiner Unterschrift:

- Ich habe keine im Merkblatt „[Zitier-Knigge](#)“ beschriebene Form des Plagiats begangen.
- Ich habe alle Methoden, Daten und Arbeitsabläufe wahrheitsgetreu dokumentiert.
- Ich habe keine Daten manipuliert.
- Ich habe alle Personen erwähnt, welche die Arbeit wesentlich unterstützt haben.

Ich nehme zur Kenntnis, dass die Arbeit mit elektronischen Hilfsmitteln auf Plagiate überprüft werden kann.

Ort, Datum

Unterschrift(en)

Blas

Bei Gruppenarbeiten sind die Namen aller Verfasserinnen und Verfasser erforderlich. Durch die Unterschriften bürgen sie gemeinsam für den gesamten Inhalt dieser schriftlichen Arbeit.